

## FREQUENCY CHARACTERISTICS OF SEISMIC REFLECTIONS FROM THIN BEDS

HAI-MAN CHUNG<sup>1</sup> AND DON C. LAWTON<sup>2</sup>

### ABSTRACT

The peak frequency characteristics of seismic reflections from a thin bed with arbitrary upper and lower normal incidence reflection coefficients is studied. Analytical results are compared to the results of numerical modelling. The comparison indicates that, except for the model where the polarities of the reflection coefficients are opposite, the peak frequency is a slowly decreasing function as the layer thickness increases. For the model with opposite polarities for the reflection coefficients, frequency tuning effects are observed at small thicknesses of the order of  $(1/16)\lambda_d$ , where  $\lambda_d$  is the predominant wavelength in the layer.

### INTRODUCTION

An important aspect of thin-bed seismic interpretation is the frequency content of a composite wavelet made up of superposed reflections from closely spaced interfaces. Widess (1973) concluded that, for the case of a single bed whose thickness is below  $(1/8)\lambda_d$ , the peak-to-trough time separation of the composite wavelet reflected from the top and bottom of the bed stays constant. However, this conclusion was based on visual inspection and is actually not analytically correct. Kallweit and Wood (1982) showed graphically that the peak-to-trough time decreases as the bed thins and stabilizes only in the limit of zero separation. In this paper, we show analytically the same result.

In our paper on the study of amplitudes of seismic reflections from thin layers (Chung and Lawton, 1995), we studied the amplitude characteristics for four reflectivities. Throughout this paper, a similar approach is taken. Peak frequency is defined as the frequency which has the maximum amplitude in the frequency domain. This contrasts with the dominant frequency, which is defined as the frequency that is derived from the wavelet peak-to-trough time. As a quantitative example, consider a Ricker wavelet centred at  $t = 0$  with peak frequency  $f_0$  (Ricker, 1940):

$$R(t) = (1 - 2\pi^2 f_0^2 t^2) e^{-\pi^2 f_0^2 t^2}$$

$$\frac{dR}{dt} = -4\pi^2 f_0^2 t e^{-\pi^2 f_0^2 t^2} - 2\pi^2 f_0^2 e^{-\pi^2 f_0^2 t^2} (1 - 2\pi^2 f_0^2 t^2). \quad (1)$$

For the wavelet peak or trough (amplitude maximum or minimum):

$$\frac{dR}{dt} = 0$$

$$\therefore -4\pi^2 f_0^2 t e^{-\pi^2 f_0^2 t^2} - 2\pi^2 f_0^2 e^{-\pi^2 f_0^2 t^2} (1 - 2\pi^2 f_0^2 t^2) = 0.$$

Simplifying, we have

$$4\pi^4 f_0^4 t^3 - 6\pi^2 f_0^2 t = 0$$

$$4\pi^2 f_0^2 t^3 - 6t = 0.$$

$t = 0$  is obviously a root, since the wavelet is centred at  $t = 0$ , which is the wavelet peak time. Therefore:

$$4\pi^2 f_0^2 t^2 = 6$$

$$t = \pm \sqrt{\frac{3}{2}} \frac{1}{\pi f_0} = \pm \frac{0.39}{f_0}.$$

The two other roots correspond to the two troughs of the wavelet, and since  $t = 0$  coincides with the wavelet peak,  $t = 0.39/f_0$  is in fact the peak-to-trough time for a Ricker wavelet. Therefore, the peak-to-trough time for a Ricker wavelet centred at  $t = 0$  is inversely proportional to the peak frequency. Hence, analyzing the peak-to-trough time behaviour and analyzing the peak frequency behaviour are

Manuscript received by the Editor July 19, 1995; revised manuscript received September 18, 1995.

<sup>1</sup>Stampeder Exploration Ltd., 1200 Eau Claire Place II, 521 3rd Avenue S.W., Calgary, Alberta T2P 3T3

<sup>2</sup>Department of Geology and Geophysics, The University of Calgary, Calgary, Alberta T2N 1N4

two different but equivalent ways of studying the same property of a wavelet. Lange and Almoghrabi (1988) studied the peak frequency behaviour of seismic reflections from thin beds as a function of bed thickness as well as the incidence angle of the seismic raypath. In this paper, an exact frequency equation and a thin-bed frequency equation are derived for the one-layer models. Transmission loss and internal multiples are ignored and dispersion is not included.

**SINGLE-LAYER MODEL**

A simple model of a thin layer embedded between two thick layers can be represented by two reflection coefficients with magnitudes  $r_1$  and  $r_2$  and traveltimes  $t_1$  and  $t_2$ , respectively, from the top of the upper thick layer (Figure 1). In general, there are four fundamentally different two-term reflectivity series, categorized as :

- Type I:  $\uparrow\downarrow$  opposite polarity and equal magnitude;
- Type II:  $\uparrow\uparrow$  equal polarity and equal magnitude;
- Type III:  $\uparrow\downarrow$  opposite polarity and unequal magnitude; and
- Type IV:  $\uparrow\uparrow$  equal polarity and unequal magnitude.

The spectrum of these reflectivity series can be expressed as:

$$X(f) = r_1 e^{i2\pi f t_1} + r_2 e^{i2\pi f t_2}$$

$$= [r_1 \cos(2\pi f t_1) + r_2 \cos(2\pi f t_2)] + i[r_1 \sin(2\pi f t_1) + r_2 \sin(2\pi f t_2)]. \tag{2}$$

The corresponding amplitude spectrum is then:

$$A(f) = \sqrt{[r_1 \cos(2\pi f t_1) + r_2 \cos(2\pi f t_2)]^2 + [r_1 \sin(2\pi f t_1) + r_2 \sin(2\pi f t_2)]^2}$$

$$= \sqrt{r_1^2 + r_2^2 + 2r_1 r_2 [\cos(2\pi f t_1) \cos(2\pi f t_2) + \sin(2\pi f t_1) \sin(2\pi f t_2)]}$$

$$= \sqrt{r_1^2 + r_2^2 + 2r_1 r_2 \cos(2\pi f \Delta t)},$$

where  $\Delta t = t_2 - t_1$  is the two-way traveltime within the thin layer.

The amplitude spectrum of a Ricker wavelet with peak frequency  $f_0$  is (Ricker, 1953):

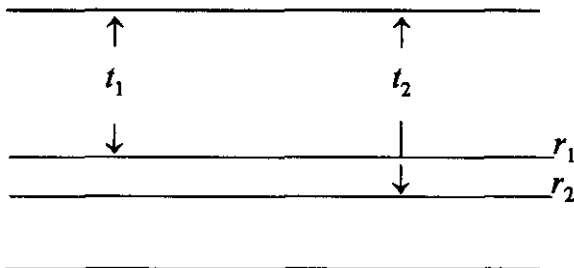


**Fig. 1.** A simple thin-layer model;  $r_1$  and  $r_2$  are reflection coefficients at each interface;  $t_1$  and  $t_2$  are 2-way traveltimes.

$$A_R(f) = \left(\frac{f}{f_0}\right)^2 e^{-\left(\frac{f}{f_0}\right)^2} \tag{3}$$

Hence, the amplitude spectrum of a composite wavelet formed by the convolution of a Ricker wavelet with a two-term reflectivity series is:

$$R(f) = A(f)A_R(f)$$

$$= \left(\frac{f}{f_0}\right)^2 e^{-\left(\frac{f}{f_0}\right)^2} \sqrt{r_1^2 + r_2^2 + 2r_1 r_2 \cos(2\pi f \Delta t)}.$$

The peak frequency can be obtained through:

$$\frac{dR(f)}{df} = \left(\frac{f}{f_0}\right)^2 e^{-\left(\frac{f}{f_0}\right)^2} \frac{-2r_1 r_2 [2\pi \Delta t \sin(2\pi f \Delta t)]}{2\sqrt{r_1^2 + r_2^2 + 2r_1 r_2 \cos(2\pi f \Delta t)}}$$

$$+ \sqrt{r_1^2 + r_2^2 + 2r_1 r_2 \cos(2\pi f \Delta t)}$$

$$\times \left[ 2\left(\frac{f}{f_0}\right) \frac{1}{f_0} e^{-\left(\frac{f}{f_0}\right)^2} + \left(\frac{f}{f_0}\right)^2 \left(-\frac{2f}{f_0}\right) \frac{1}{f_0} e^{-\left(\frac{f}{f_0}\right)^2} \right] = 0.$$

Simplifying and using  $f_p$  to denote peak frequency results in:

$$f_p [r_1 r_2 \pi \Delta t \sin(2\pi f_p \Delta t)] = [r_1^2 + r_2^2 + 2r_1 r_2 \cos(2\pi f_p \Delta t)] \left[ 1 - \left(\frac{f_p}{f_0}\right)^2 \right]. \tag{4}$$

where  $f_p$  is the peak frequency sought. Equation (4) is called the exact peak frequency equation and  $f_p$  can be solved iteratively. Also, equation (4) can be used for both normal incidence and nonnormal incidence cases, i.e., in general,  $r_1$  and  $r_2$  may be offset-dependent.

Equation (4) can also be approximated by assuming that  $\Delta t$  is sufficiently small so that

$$\sin(2\pi f_p \Delta t) \approx 2\pi f_p \Delta t \text{ and } \cos(2\pi f_p \Delta t) \approx 1,$$

$$f_p r_1 r_2 \pi \Delta t (2\pi f_p \Delta t) = (r_1^2 + r_2^2 + 2r_1 r_2) \left[ 1 - \left(\frac{f_p}{f_0}\right)^2 \right]$$

$$f_p^2 (2r_1 r_2 \pi^2 \Delta t^2) = k^2 \left[ 1 - \left(\frac{f_p}{f_0}\right)^2 \right]$$

where

$$k^2 = r_1^2 + r_2^2 + 2r_1r_2 = (r_1 + r_2)^2.$$

Rearranging terms, we have

$$f_p^2 \left[ 2r_1r_2\pi^2\Delta t^2 + \frac{k^2}{f_0^2} \right] = k^2$$

$$f_p^2 = \frac{k^2 f_0^2}{2r_1r_2\pi^2\Delta t^2 f_0^2 + k^2}$$

or

$$f_p = f_0 \left[ 1 + \frac{2\pi^2 r_1 r_2 f_0^2 \Delta t^2}{k^2} \right]^{-1/2}$$

$$\therefore f_p \approx f_0 \left[ 1 - \frac{\pi^2 \Delta t^2 f_0^2 r_1 r_2}{k^2} \right], \quad (5)$$

assuming  $\pi^2 \Delta t^2 f_0^2 r_1 r_2 \ll k^2$ .

Equation (5) is defined here as the thin-bed peak frequency equation, since  $\Delta t$  is assumed to be very small. Since  $k^2$  is always positive, equation (5) indicates that, if a Ricker wavelet is convolved with a two-term reflectivity sequence whose terms are separated by a small time interval, then the peak frequency of the composite wavelet will decrease as  $\Delta t$  increases if  $r_1$  and  $r_2$  are of the same polarity, and vice versa if  $r_1$  and  $r_2$  are of opposite polarities. We show that equation (5) is a good approximation for Types II and IV reflectivity sequences, but less appropriate for Types I and III cases. If  $r_1$  and  $r_2$  are of opposite polarities but close in magnitude,  $k$  can be very small, resulting in an abnormally large value for  $f_p$  in equation (5). For the case where  $r_2 = -r_1$  (Type I reflectivity), equation (5) is invalid because of the singularity due to  $k = 0$ . However, for this case we put  $r_2 = -r_1$  in equation (4), yielding:

$$f \left[ -r_1^2 \pi \Delta t \sin(2\pi f_p \Delta t) \right] = \left[ 2r_1^2 - 2r_1^2 \cos(2\pi f_p \Delta t) \right] \left[ 1 - \left( \frac{f_p}{f_0} \right)^2 \right]$$

$$-f \pi \Delta t \sin(2\pi f_p \Delta t) = 2 \left[ 1 - \cos(2\pi f_p \Delta t) \right] \left[ 1 - \left( \frac{f_p}{f_0} \right)^2 \right]$$

$$= 2 \left[ 2 \sin^2(\pi f_p \Delta t) \right] \left[ 1 - \left( \frac{f_p}{f_0} \right)^2 \right]$$

$$= 4 \sin^2(\pi f_p \Delta t) \left[ 1 - \left( \frac{f_p}{f_0} \right)^2 \right].$$

Making the thin-bed approximation  $\sin(2\pi f_p \Delta t) \approx 2\pi f_p \Delta t$  for small  $\Delta t$ , we have:

$$f_p^2 2\pi^2 \Delta t^2 = 4\pi^2 f_p^2 \Delta t^2 \left[ \left( \frac{f_p}{f_0} \right)^2 - 1 \right]$$

$$\left( \frac{f_p}{f_0} \right)^2 - 1 = \frac{1}{2}$$

$$\therefore f_p = \sqrt{\frac{3}{2}} f_0. \quad (6)$$

This is identical to the results obtained by Lange and Almoghrabi (1988) although the approach used in this paper is different. Lange and Almoghrabi (1988) followed the conclusion of Widess (1973) and assumed that a reflected composite wavelet takes the shape of the derivative of the source wavelet when the bed thins to  $(1/8)\lambda_d$ , and this shape remains constant as the bed continues to thin to zero thickness. They then took the first derivative with respect to time of the amplitude spectrum of a Ricker wavelet and solved for the new peak frequency. In the approach presented in this paper, there is no assumption about the shape of the reflected composite wavelet, regardless of the thickness of the bed; the only assumption is that the bed has to be sufficiently thin for the thin-bed assumption to be valid. Furthermore, we show that the calculated peak frequency does not occur when the bed thickness is equal to  $(1/8)\lambda_d$  as suggested by Widess (1973) and Lange and Almoghrabi (1988), but it is actually the limiting value for the peak frequency as the bed thickness approaches zero. Indirectly, this limiting behaviour also agrees with the conclusion of Kallweit and Wood (1982) about the limiting behaviour of the peak-to-trough time.

Combining the results of Widess (1973), Lange and Almoghrabi (1988) and the results deduced from equation (4), it is concluded that as the thickness of a thin bed represented by a Type I reflectivity sequence decreases, the peak frequency of the reflected composite wavelet will increase. As the thickness of the bed reduces to the limiting value of zero, the shape of the reflected composite wavelet will approach the shape of the derivative of the source wavelet, and the limiting peak frequency value is given by  $\sqrt{3/2} f_0$  where  $f_0$  is the peak frequency of the source Ricker wavelet.

## RESULTS, NORMAL INCIDENCE, SINGLE-LAYER MODEL

To study the peak frequency response of a thin bed to vertically-incident plane waves, a simple wedge model (Figure 2) was used. Densities and velocities used for the models that

represent the four types of reflectivities are listed in Table 1. The velocities were chosen to be typical of lower Cretaceous formations in southern Alberta and the densities were calculated from the velocities using the equation of Gardner et al. (1974). For all four models, the reflection coefficients of the upper and lower interfaces are referred to as  $r_1$  and  $r_2$ , respectively. The geometry of the wedge model was set up so that the trace number in the synthetic seismograms is equal to the thickness of the wedge in metres at the trace location. Because of the thickness of interest, the number of traces plotted for each synthetic seismogram will extend to only two to three metres more than the  $(1/4)\lambda_d$  value.

Synthetic seismograms were generated by convolving a Ricker wavelet (3 frequencies are shown) with a two-term reflectivity series. In each model, the amplitude of the Ricker wavelet was scaled by the reflection coefficient at each interface. A zero-phase wavelet is chosen because a zero-phase wavelet gives the maximum vertical resolution compared to other phases, as shown by Berkhout (1984). All seismograms were generated with a sampling interval of 0.1 ms. Synthetic seismograms for four different wedge models (Table 1) are shown in Figure 3. In this example, a 31-Hz Ricker wavelet was used since this is a typical peak frequency of seismic data in the Western Canada Sedimentary Basin. For each seismogram generated, the peak frequency of each trace was obtained by the maximum amplitude of its Fourier spectrum and these frequencies were compared to those values predicted from equations (4) and (5).

For both Type I and Type II reflectivity studies, three input peak frequencies were used, the purpose being to verify that the equations are frequency-independent. For Types III and IV reflectivities, only the results obtained for a 31-Hz Ricker source wavelet are presented. The presented results are valid for the specific models used and may not be valid for similar reflectivity sequences whose reflection coefficients have significantly different magnitudes. However, equation (4) can always be used to study more different types of models.

**Type I reflectivity**

Figure 4 is a plot of the results of equation (4) for this model for three different input Ricker wavelets with peak frequencies of 18 Hz, 31 Hz and 50 Hz. The exact peak frequency equation was solved by iteration and results compared to those derived from modelling.

Figure 4 shows that values predicted by equation (4) agree exactly with values from numerical modelling for the three

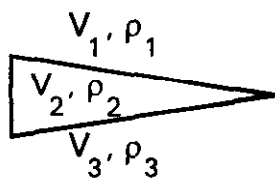


Fig. 2. A wedge model;  $V_1$ ,  $V_2$  and  $V_3$  are the P-wave velocities;  $\rho_1$ ,  $\rho_2$  and  $\rho_3$  are the densities.

Table 1. Lithologies, layer velocities, layer densities and reflection coefficients for four models.

Types of Reflectivity Series	Above Wedge $V_1$ (m/s) $\rho_1$ (kg/m <sup>3</sup> )	Wedge $V_2$ (m/s) $\rho_2$ (kg/m <sup>3</sup> )	Below Wedge $V_3$ (m/s) $\rho_3$ (kg/m <sup>3</sup> )	$r_1$	$r_2$
I	nonporous sand 4270 2505	porous sand 3050 2303	nonporous sand 4270 2505	-0.2072	0.2072
II	porous sand 3050 2303	silt 3560 2395	nonporous sand 4270 2505	0.1047	0.1047
III	silt 3800 2434	porous sand 3050 2303	nonporous sand 4270 2505	-0.1371	0.2072
IV	porous sand 3050 2303	shale 3350 2359	nonporous sand 4270 2505	0.0596	0.1494

different frequencies used. This implies that the peak frequency equation is independent of frequency. The results show that, for Type I reflectivity, the peak frequency of the composite reflected wavelet decreases monotonically as the bed thickness increases. However, the gradient is nonlinear and is frequency-dependent. For example, when the wedge thickness increases from 1 m to 13 m, the peak frequency decreases by about 2% for  $f_0 = 18$  Hz and about 14% for  $f_0 = 50$  Hz. In all cases, however, the peak frequency is always greater than the input frequency for  $b/\lambda_d < 0.4$

**Type II reflectivity**

For this reflectivity sequence, the results from both the exact peak frequency equation and the thin-bed approximation agree well with the modelling results (Figure 5). Both results are frequency-independent. Since the exact peak frequency equation does not contain any approximations, it is expected to agree with the modelling results for all thicknesses. However, the results from the thin-bed peak frequency equation will agree with the modelling results only for thicknesses for which the thin-bed approximation remains valid. In Figure 5, the approximate and exact results start to deviate at thickness greater about  $0.23\lambda_d$  for all three frequencies tested, although the error is relatively small.

**Type III reflectivity**

Chung and Lawton (1995) showed that Type III reflectivity can be expressed as the sum of Types I and II reflectivities. Since the peak frequencies for both Type I and II reflectivities increase slowly as the bed thickness decreases, similar behaviour may be expected of Type III reflectivity. However, the data plotted in Figure 6 show that, as the thickness of the wedge increases, the calculated exact peak frequency of the reflected composite wavelet first increases, reaches a maximum at about  $0.09\lambda_d$ , and then slowly decreases. This behaviour is observed only for Type III reflectivity among the four types of reflectivities studied. Numerical modelling results are identical to those predicted from equation (4).

The results from the thin-bed peak frequency equation agree with the modelling results for thickness only up to

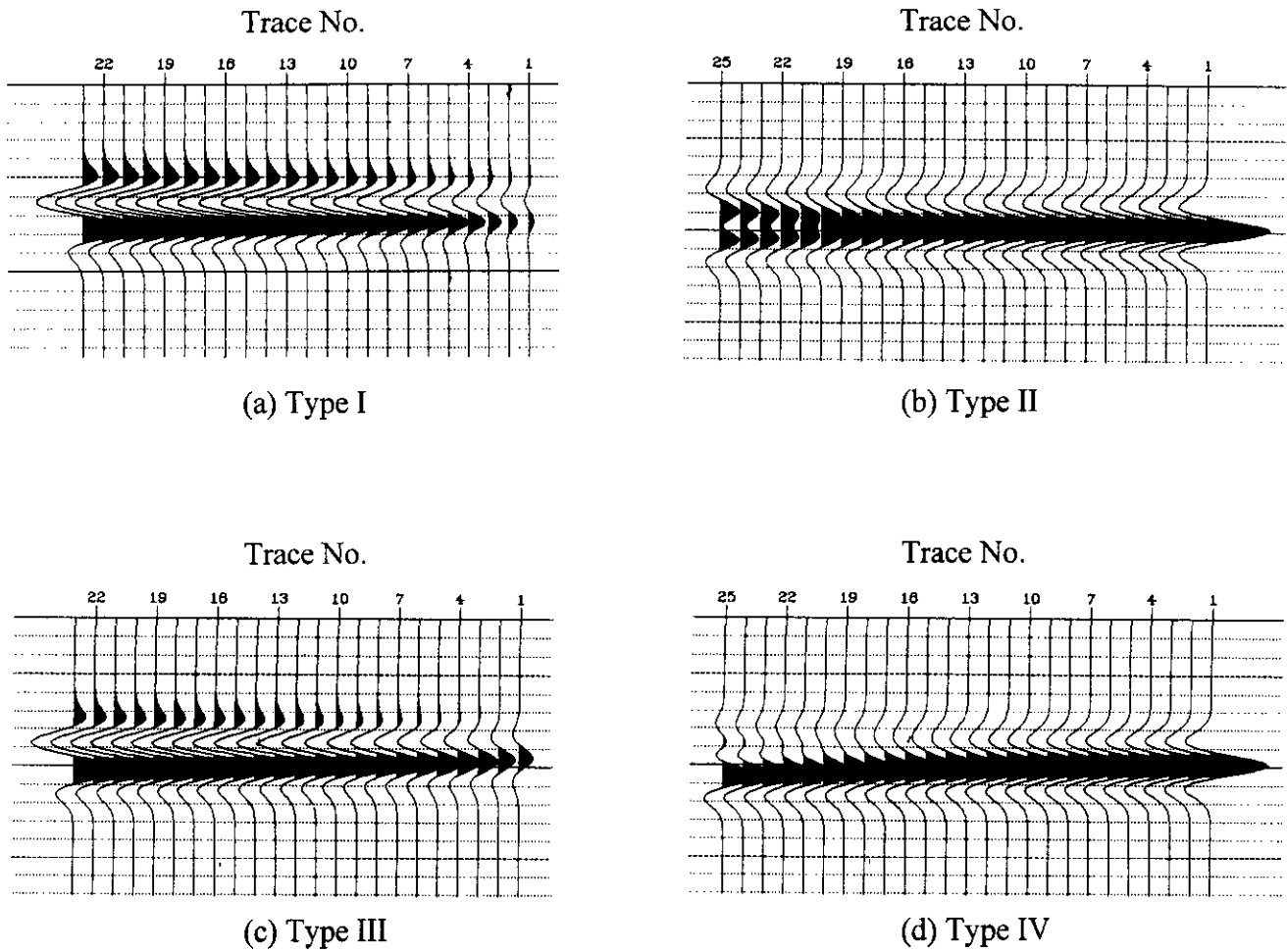


Fig. 3. Synthetic seismograms for (a) Type I, (b) Type II, (c) Type III and (d) Type IV reflectivities. The source wavelet is a 31-Hz Ricker wavelet and the arrows indicate the  $(1/8)\lambda_d$  and  $(1/4)\lambda_d$  locations. Timing lines are at 10-ms intervals.

about  $0.03\lambda_d$ . Above this thickness, the peak frequency values increase sharply and diverge rapidly from the modelling results. As explained earlier, the reason is the small numerical value of the factor  $(r_1+r_2)$  in the denominator of equation (5). For the Type III reflectivity model used in this paper,  $(r_1+r_2) = 0.0702$ . For example, this is almost three times smaller than the value of 0.2098 for Type II reflectivity model.

**Type IV reflectivity**

For this reflectivity sequence, the behaviour of the peak frequency of the reflected composite wavelet is similar to that for Types I and II reflectivities. Figure 7 shows the results for a 31-Hz Ricker wavelet as the source wavelet. Both the exact peak frequency equation and the thin-bed peak frequency equation lead to results which are consistent

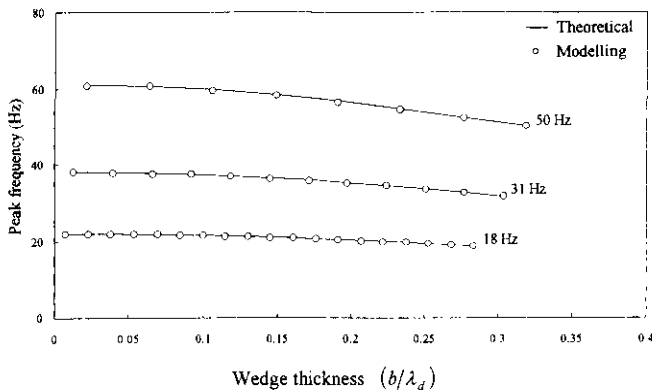


Fig. 4. Peak frequency versus thickness for Type I reflectivity ( $\perp$ ).

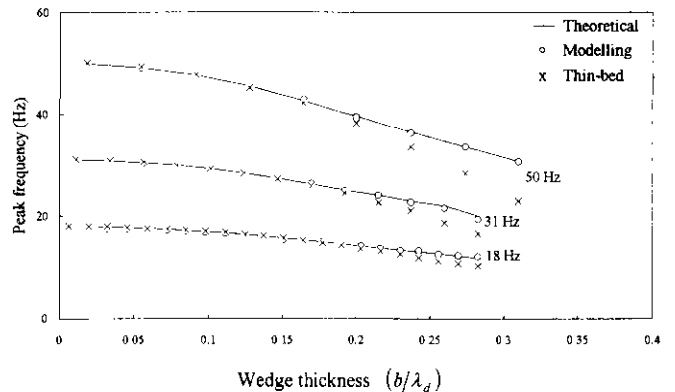


Fig. 5. Peak frequency versus thickness for Type II reflectivity ( $\parallel$ ).

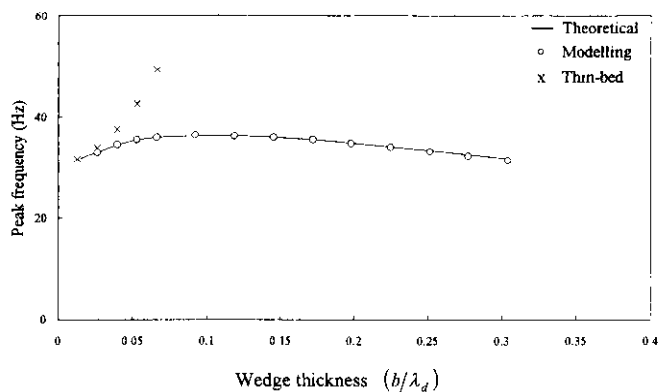


Fig. 6. Peak frequency versus thickness for Type III reflectivity ( $\perp$ ).

with the modelling results. They all indicate that the peak frequency decreases slowly as the thickness of the wedge increases.

DISCUSSION

Both the exact peak frequency equation [equation (4)] and the thin-bed peak frequency equation [equation (5)] have been developed for the single-layer models. Equation (4) gives exact values for the peak frequency of seismic reflections from a two-term reflectivity series. However, when the thin-bed assumption is valid, this equation reduces to a much simpler expression, i.e., equation (5), which can be used to predict the behaviour of the peak frequency as a function of thickness in a qualitative manner.

In stratigraphic interpretation of seismic data, emphasis traditionally has always been placed on the amplitude of the reflected wavelet, whereas its frequency behaviour has not been widely used. This is probably due to the fact that variations in amplitude can be related to variations in physical properties such as the velocity and density through the definition of the reflection coefficient in a straightforward manner. By contrast, relationships between the peak frequency of a reflected wavelet and any properties of a geological formation have not yet been firmly established.

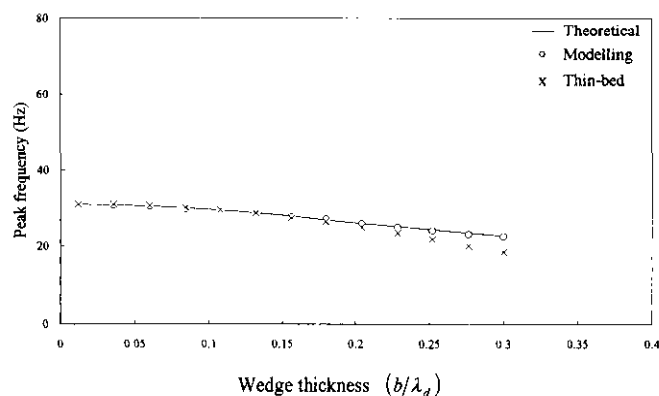


Fig. 7. Peak frequency versus thickness for Type IV reflectivity ( $\perp$ ).

From the analysis of the single-layer models, several conclusions can be drawn. The analysis shows that Type I reflectivity is a singular case in its peak frequency behaviour in that, as the bed thickness approaches zero, it is the only two-term reflectivity for which the peak frequency of its reflected composite wavelet approaches the value of the peak frequency of the derivative of the source wavelet, which is equal to  $\sqrt{3/2}f_0$ , where  $f_0$  is the peak frequency of the source wavelet. However, at zero thickness, there is no reflection and the peak frequency curves in Figure 4 should have the same values as the peak frequencies of the source wavelets. Thus, there is a discontinuity at zero thickness for the peak frequency curves of Type I reflectivity.

For Types II, III and IV reflectivity series, as the layer thickness approaches zero, the peak frequencies approach the values of the peak frequencies of the source wavelets. Furthermore, the Type III reflectivity is the only reflectivity that exhibits frequency tuning effect at approximately the  $0.1\lambda_d$  thickness. Thus, in a geological setting which can be modelled by a single thin bed, if the seismic data shows a frequency tuning effect, the setting can probably be represented by a Type III reflectivity sequence.

In processing seismic data collected over thin geological formations, geophysicists often attempt to increase the high-frequency content of the data to increase its vertical resolution. The results shown in Figure 4 indicate that, even if the thickness is below resolution, higher frequencies are still preferable because they are more sensitive to changes in bed thickness than are lower frequencies.

Equation (4) and (5) can be used for forward modelling and the results can then be compared to observed results from seismic data. If the two sets of results differ significantly, parameters can then be selectively modified in equations (4) and (5) until a match is obtained. This will assist the geophysicists in the interpretation process in identifying the possible geological changes that contribute to any observed changes or anomalies in seismic data.

REFERENCES

Berkhout, A.J., 1984, Seismic resolution: handbook of geophysical exploration: Section I, Vol. 12, chap. II, Geophysical Press.  
 Chung, H. and Lawton, D.C., 1995, Amplitude responses of thin beds: sinusoidal approximation versus Ricker approximation: *Geophysics* **60**, 223-230.  
 Gardner, G.H.F., Gardner, L.W. and Gregory, A.R., 1974, Formation velocity and density - the diagnostic basis for stratigraphic traps: *Geophysics* **39**, 770-780.  
 Kallweit, R.S. and Wood, L.C., 1982, The limits of resolution of zero-phase wavelets: *Geophysics* **47**, 1035-1046.  
 Lange, J. and Almoghrabi, H., 1988, Lithology discrimination for thin layers using wavelet signal parameters: *Geophysics* **53**, 1512-1519.  
 Ricker, N., 1940, The form and nature of seismic waves and the structure of seismograms: *Geophysics* **5**, 348-366.  
 \_\_\_\_\_, 1953, Wavelet contraction, wavelet expansion, and the control of seismic resolution: *Geophysics* **18**, 769-792.  
 Widess, M.B., 1973, How thin is a thin bed?: *Geophysics* **38**, 1176-1180.